

See discussions, stats, and author profiles for this publication at: <https://www.researchgate.net/publication/336601353>

Terahertz shielding properties of aero-GaN

Article in *Semiconductor Science and Technology* · October 2019

DOI: 10.1088/1361-6641/ab4e58

CITATIONS

0

READS

61

13 authors, including:



Tudor Braniste

Technical University of Moldova

41 PUBLICATIONS 267 CITATIONS

[SEE PROFILE](#)



Liudmila Alyabyeva

Moscow Institute of Physics and Technology

22 PUBLICATIONS 57 CITATIONS

[SEE PROFILE](#)



Vladimir Ciobanu

Technical University of Moldova

10 PUBLICATIONS 46 CITATIONS

[SEE PROFILE](#)

Martino Aldrigo

National Institute for Research and Development in Microtechnologies - IMT Buch...

48 PUBLICATIONS 228 CITATIONS

[SEE PROFILE](#)

Some of the authors of this publication are also working on these related projects:



Stimuli responsive materials in applications [View project](#)



material science and nanotechnology [View project](#)

LETTER • **OPEN ACCESS**

Terahertz shielding properties of aero-GaN

To cite this article: Tudor Braniste *et al* 2019 *Semicond. Sci. Technol.* **34** 12LT02

View the [article online](#) for updates and enhancements.










IOP | ebooksTM

Bringing you innovative digital publishing with leading voices to create your essential collection of books in STEM research.

Start exploring the **collection** - download the first chapter of every title for free.

Letter

Terahertz shielding properties of aero-GaN

Tudor Braniste¹ , Sergey Zhukov², Mircea Dragoman³ ,
Liudmila Alyabyeva² , Vladimir Ciobanu¹, Martino Aldrigo³ ,
Daniela Dragoman⁴ , Sergiu Iordanescu³ , Sindu Shree⁵,
Simion Raevschi⁶, Rainer Adelung⁵, Boris Gorshunov² and
Ion Tiginyanu^{1,7,8} 

¹ National Center for Materials Study and Testing, Technical University of Moldova, Stefan cel Mare av. 168, Chisinau 2004, Moldova

² Laboratory of Terahertz Spectroscopy, Moscow Institute of Physics and Technology, Dolgoprudny 141701, Moscow region, Russia

³ National Institute for Research and Development in Microtechnologies (IMT Bucharest), Erou Iancu Nicolae 126A, Voluntari 077190, Romania

⁴ Univ. of Bucharest, Physics Faculty, PO Box MG-11, Bucharest 077125, Romania

⁵ Institute for Materials Science, University of Kiel, Kaiserstr. 2, Kiel D-24143, Germany

⁶ Department of Physics and Engineering, State University of Moldova, Alexei Mateevici str. 60, Chisinau 2009, Moldova

⁷ Academy of Sciences of Moldova, Stefan cel Mare av. 1, Chisinau 2004, Moldova

E-mail: tudor.braniste@cnstm.utm.md and tiginyanu@asm.md

Received 15 August 2019, revised 26 September 2019

Accepted for publication 16 October 2019

Published 4 November 2019



Abstract

The electrodynamic properties of the first aero-material based on compound semiconductor, namely of Aero-GaN, in the terahertz frequency region are experimentally investigated. Spectra of complex dielectric permittivity, refractive index, surface impedance are measured at frequencies 4–100 cm⁻¹ and in the temperature interval 4–300 K. The shielding properties are found based on experimental data. The aero-material shows excellent shielding effectiveness in the frequency range from 0.1 to 1.3 THz, exceeding 40 dB in a huge frequency bandwidth, which is of high interest for industrial applications. These results place the aero-GaN among the best THz shielding materials known today.

Keywords: aero-GaN, complex dielectric permittivity, THz shielding

(Some figures may appear in colour only in the online journal)

1. Introduction

Terahertz (THz) radiation, ranging from 100 GHz up to 30 THz, is perceived as an electromagnetic spectrum region with rather weak radiation sources. This statement illustrates

the narrow perception of this spectral region, originating from the lack of miniaturized semiconductor sources able to generate tunable and medium- or high-level electromagnetic power, as in microwaves and millimeter wave regions. However, there are strong THz radiation sources such as far-infrared lasers, gyrotrons, backward-wave oscillators (BWOs) [1, 2], free-electron lasers or synchrotrons. Even the miniaturized semiconductor THz sources show nowadays rather large THz emitted powers. For example, an array of 89 resonant-tunneling diodes integrated with dipole antennas generates 0.73 mW at 1 THz [3]; the BWOs provide coherent and continuously tunable radiation in the range between

⁸ Author to whom any correspondence should be addressed

0.03 THz and up to 1.4 THz, with output power of several hundreds of milliWatts at low frequencies and about 1 mW at high frequencies. There are already amplifiers, such as InP-based high electron mobility transistor, able to amplify at 1 THz at room temperature [4, 5]. THz wireless communications are a hot topic [6] and already serious concerns about public health are raised [7].

Therefore, various materials are searched today to protect both equipment and human beings against unwanted THz radiation, since biological effects of such radiations may be dangerous [8]. Electromagnetic interference (EMI) shielding materials for THz spectrum are now dominated by carbon-based nanomaterials, such as carbon nanotubes [9, 10], and graphene [11], which are very often mixed with polymers, thus forming nanocomposites. A recent review regarding EMI shielding of carbon-based nanomaterials is found in [12].

In this paper, we investigate the THz EMI shielding properties of the aerogalnite (aero-GaN) which is a new ultra-porous semiconductor nanomaterial formed by an interconnected network of hollow GaN microtetrapods (with the wall thickness in the nanometer scale). The fabrication method and its physical properties are described in detail in [13].

2. Experimental

GaN microtetrapods were fabricated as follows. Ultrathin layers of GaN have been grown on sacrificial ZnO microtetrapods, with arms diameter of 2–10 μm and lengths from 20 to 100 μm . The growth process occurs in a hydride vapor phase epitaxy system, which is equipped with a four-temperature-zone-heated horizontal reactor. In the source zone, at 850 °C, gallium chloride is formed as a result of chemical reactions between gaseous hydrogen chloride and liquid gallium. The formed GaCl interacts with gaseous NH_3 in the reaction zone and initiates the GaN growth process at 600 °C for 10 min, followed by another 10 min growth at 850 °C, when the GaN layer is grown uniformly on the surface of ZnO microtetrapods. The flow rates for HCl, NH_3 and H_2 equals to 15 sml min^{-1} , 600 sml min^{-1} and 3600 sml min^{-1} , respectively. Note that at the growth temperature, GaN deposition is accompanied by simultaneous gradual decomposition and removal of the underneath ZnO template, which occurs due to harsh reaction corrosive conditions. The density of ZnO microtetrapods in the initial interconnected network was 0.3 g cm^{-3} , which decreased about 20 times after GaN growth and ZnO removal. Figure 1 depicts the SEM images of the aerogalnite sample at different magnifications. An optical image of the aerogalnite sample under investigation is presented in the inset of figure 1(a), while a single hollow microtetrapod of GaN is presented in the figure 1(c).

For the terahertz characterization of the material, a bulk sample was prepared in the form of a layer of 1.3 mm in thickness and of about 1 cm in diameter. The layer was fixed inside a brass ring between two stretched polyethylene films with a thickness of 8 μm (see figure 1). We have additionally investigated a slightly denser (by about 12%) sample that was

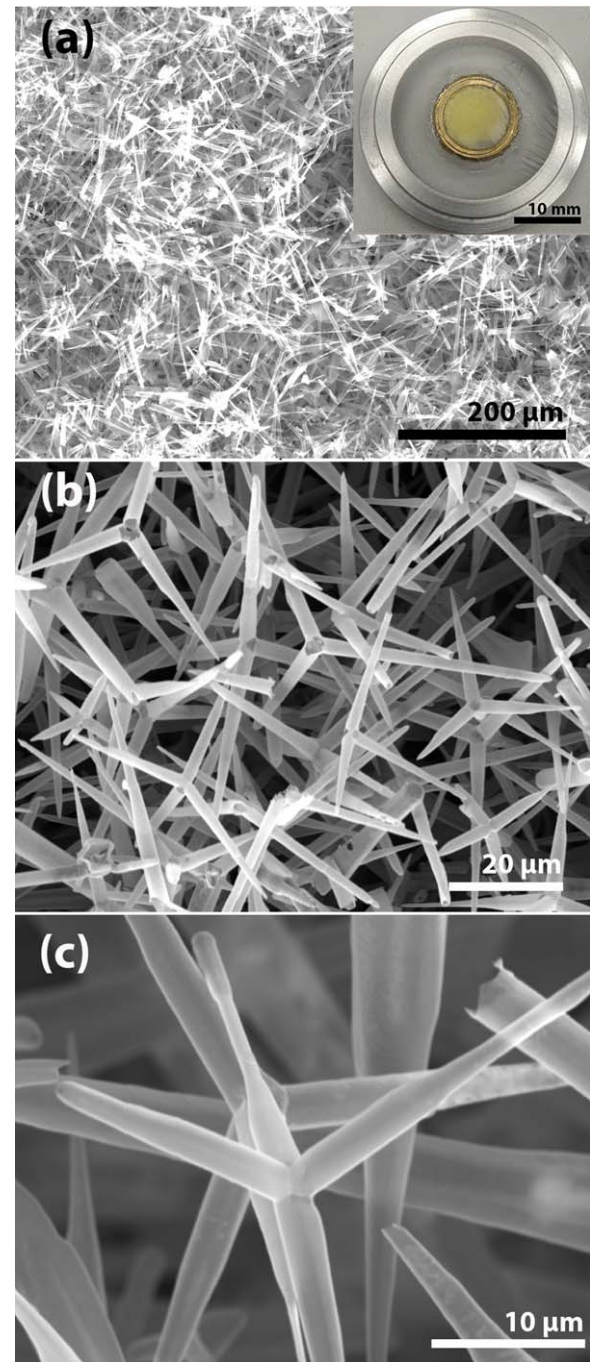


Figure 1. SEM images of the interconnected network of aero-GaN hollow microtetrapods at different magnifications. The inset in (a) shows the optical image of the aerogalnite sample in the THz measurement holder.

prepared by gentle pressing the as-grown material between two plane surfaces. THz spectra of complex dielectric permittivity $\varepsilon^*(\nu) = \varepsilon'(\nu) + i\varepsilon''(\nu)$ were measured with the help of commercial time-domain spectrometer TeraView TPS 3000. The measurements were realized in the range $\nu = 4\text{--}100\text{ cm}^{-1}$ and temperature interval T from 4 K to 300 K. The spectra of real and imaginary permittivity are determined directly in the transmission geometry via measurements of the complex transmission coefficient (amplitude and phase) of the plane-parallel samples (Note that at the

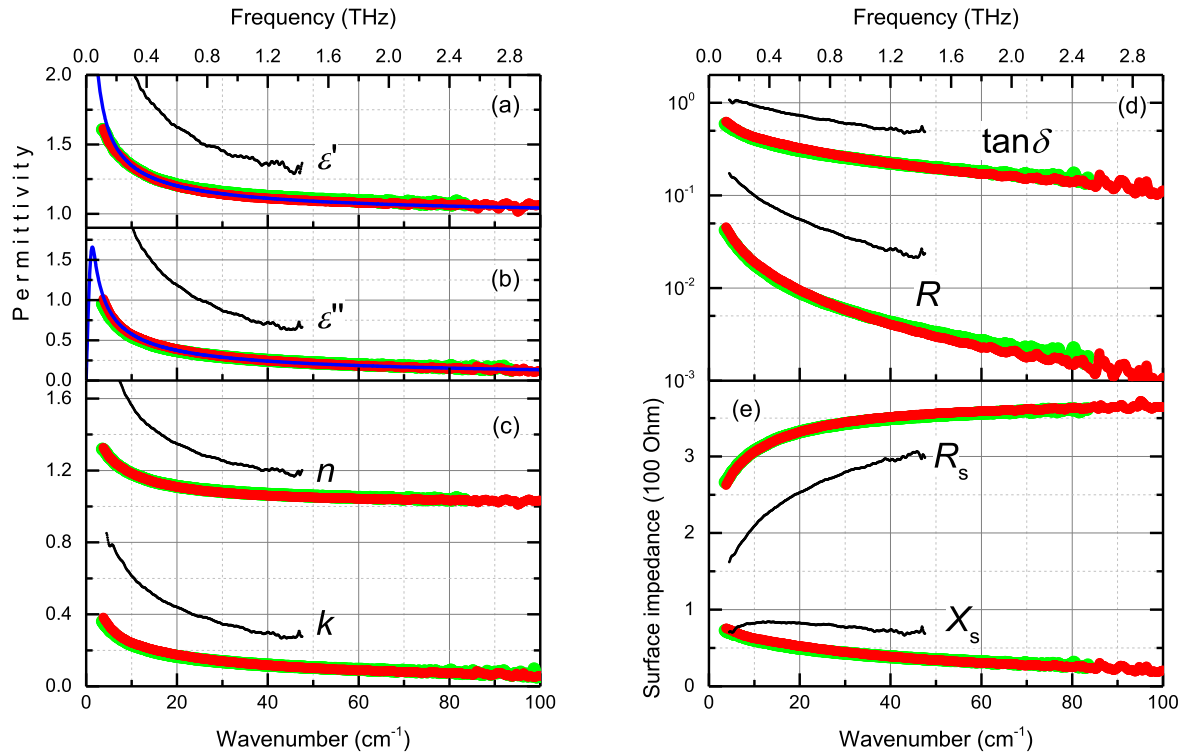


Figure 2. Terahertz spectra of the electrodynamic characteristics of the as grown and slightly densified samples of aerogalnite: real ε' (a) and imaginary ε'' (b) parts of dielectric permittivity; real n and imaginary k parts (c) of refractive index; dielectric loss tangent $\tan \delta$ and reflectivity R (d); real R_s and imaginary X_s parts of surface impedance (e). Red curves correspond to the temperature $T = 300$ K, green curves correspond to $T = 4$ K. The curves of the densified samples are given in black. Blue lines in panels (a) and (b) show the least-square fits to the spectra based on the Havriliak–Nagami equation (1); parameters of the fit are given in the text.

mentioned frequencies the polyethylene films practically do not affect the spectra). Low-temperature measurements were realized using a home-made helium-flow cryostat equipped with polypropylene windows.

3. Results and discussion

Figures 2(a) and (b) show the spectra of real and imaginary parts of dielectric permittivity of as-grown sample measured at room temperature and at $T = 4$ K. Only a weak temperature dependence of the THz response is detected. The spectra demonstrate a pronounced relaxational behavior, typical for disordered materials, and were processed using the empirical Havriliak–Nagami expression:

$$\varepsilon^*(\nu) = \varepsilon_\infty + \Delta\varepsilon[1 + (2\pi\nu\tau)^{1-\alpha}]^{-\beta}, \quad (1)$$

where $\Delta\varepsilon$ is the relaxation strength, $\tau = (2\pi\nu_R)^{-1}$ is the relaxation time, ν_R is the relaxation frequency, α and β characterize asymmetry and broadness of the relaxation peak, respectively, and ε_∞ is the high-frequency dielectric constant. The results of the fit obtained for $T = 300$ K are shown by solid lines in figures 2(a) and (b). The corresponding values of the Havriliak–Nagami parameters are collected in table 1. When the sample is cooled from 300 to 4 K, an increase of the relaxation time (corresponding to a decrease of the relaxation frequency) can be observed, thus indicating a slowing down of the relaxation process. The parameters α and β remain

Table 1. Parameters of the Havriliak–Nagami model, equation (1), obtained by fitting terahertz spectra of real and imaginary permittivity of a network of aero-GaN hollow microtetrapods measured at two temperatures, $T = 300$ K and $T = 4$ K: relaxation strength $\Delta\varepsilon$, relaxation time $\tau = (2\pi\nu_R)^{-1}$, relaxation frequency ν_R , coefficients α and β that characterize asymmetry and broadness of the relaxation peak, respectively, and high-frequency dielectric constant ε_∞ .

T (K)	$\Delta\varepsilon$	τ , ns	ν_R , cm^{-1} (GHz)	α	β	ε_∞
300	6.65	0.1	0.31 (9.4)	0.16	0.77	1
4	8.43	0.2	0.16 (4.8)	0.17	0.74	1

practically unchanged. It should be noted that in the studied frequency interval, i.e. from 4 to 100 cm^{-1} , there must be two mechanisms contributing to the observed relaxation-like THz dispersion. At the highest frequencies, the probing radiation wavelength becomes comparable to the characteristic length scale of the studied sample constituents (hollow tetrapods): the frequency of 100 cm^{-1} corresponds to the wavelength $\lambda = 100 \mu\text{m}$. One thus expects an increasing role of scattering effects when the frequency is enhanced towards the high-frequency end of the used frequency interval. At the low-frequency end, the radiation wavelength far exceeds the size of the sample inhomogeneities: for example, the lowest frequency of 4 cm^{-1} corresponds to the wavelength $\lambda = 2.5 \text{ mm}$. As a result, during frequency increase from 4 to

100 cm^{-1} there would be a ‘crossover’ of the observed relaxational behavior of the dielectric spectra that are determined mainly by the effective medium-type response at low frequencies and mainly by scattering of the radiation by sample inhomogeneities at high frequencies. It is the joint contribution of these two mechanisms that makes it necessary to use equation (1) in its most general form when the value of α is different from zero and the value of β is different from one; note that the simplest case with $\alpha = 0$ and $\beta = 1$ corresponds to the Debye-like relaxation.

The origin of the pronounced dispersion observed in the spectra below $20\text{--}30\text{ cm}^{-1}$ (where scattering is not dominating) should be connected with the polarizability of the 3D architecture of mutually interpenetrated GaN aerotetrapods of the studied material. III–V nitrides, including GaN, are known for their unusually strong polarizability, both spontaneous and piezoelectric [14–16]. We thus expect that the arms of the hollow aerotetrapods can acquire electrical polarization on their walls during deformations and/or stresses. Additional polarization can be generated at intersections or at ZnO–GaN interfaces, though the content of residual zinc oxide is not high (3%–4%). Since the detected relaxation frequency, of just few GHz (see table 1), is rather low, we believe that the main contribution to the process comes from dynamics of relatively big complexes involving certain number of tetrapods.

In figure 2 we present also the spectra of some additional electromagnetic characteristics of the studied material, that are useful for assessing possibilities of their use in various applications: real n and imaginary k parts of the refractive index $n^* = n + ik$ (c), loss tangent $\tan\delta = \epsilon''/\epsilon'$, bulk reflectivity $R = [(n - 1)^2 + k^2]/[(n + 1)^2 + k^2]$ (d) and real $R_S = \frac{4\pi}{c} \frac{n}{n^2 + k^2}$ and imaginary $X_S = \frac{4\pi}{c} \frac{k}{n^2 + k^2}$ parts of surface impedance (e). Note the small value of the reflectivity, which is basically determined by the low value of the real refractive index that is close to 1 due to, both, radiation scattering effect and low density of the material. Densified sample is characterized by larger values of all measured quantities except the surface reactance X_S .

The effective THz EMI shielding properties of the proposed aero-GaN can be studied by extracting the corresponding shielding effectiveness (SE), which accounts for two major contributions: shielding by reflection (SER) and shielding by absorption (SEA). In particular, SE is the 10-base logarithm of the ratio of the incident power I (or transmitted power T in absence of any shield, i.e. the aero-GaN). However, the two terms SER and SEA strongly depend on the reflected power (R) and the absorbed power $A = I - (T + R)$, respectively. We assume that R also comprises the effect of multiple reflections (i.e. the reflections occurring inside the shielding material due to internal scattering of the EM waves) [17], which decreases the overall EMI SE. However, since the thickness of the sample is greater than the skin depth at the lowest frequency considered for the calculation of the EMI SE (at 0.123 THz , the skin depth is about $450\text{ }\mu\text{m}$), the contribution of the multiple reflections is negligible. The

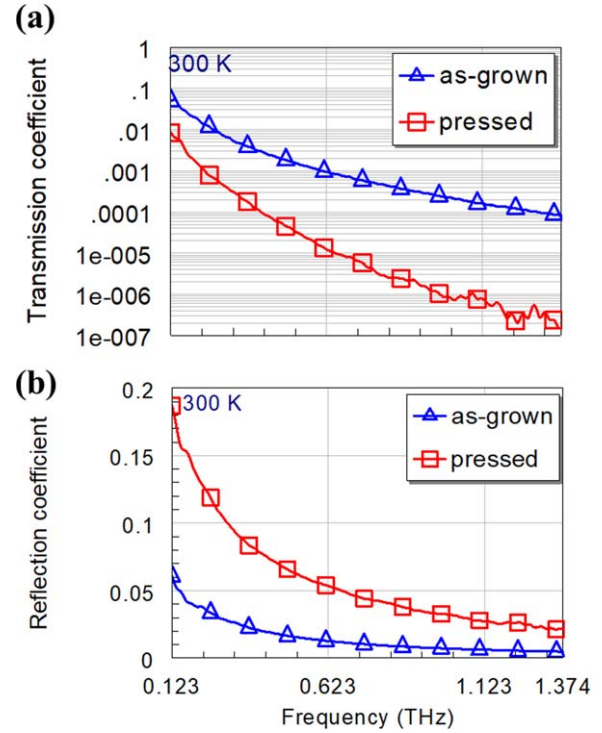


Figure 3. Measured (a) transmission and (b) reflection coefficient versus frequency at room temperature ($T = 300\text{ K}$), for the aero-GaN as-grown and pressed.

equations used for the overall SE are the following [18]:

$$\text{SE} = \text{SER} + \text{SEA} = 10 \log \frac{I}{T}, \quad (2a)$$

$$\text{SER} = 10 \log \frac{I}{I - R}, \quad (2b)$$

$$\text{SEA} = 10 \log \frac{I - R}{T}. \quad (2c)$$

Recently, the EMI shielding properties of aero-GaN in X band have been demonstrated [19]: at microwaves, the main contribution is due to SER, since the electrical conductivity of the material is of the order of hundreds up to thousands of S/m. In the THz region, one can expect that the principal shielding mechanism is due to the absorption of incoming electromagnetic radiation. First, in figure 3 we show the results of measurements of transmission and reflection coefficients (for as-grown and pressed aero-GaN) plotted versus frequency (in THz) at $T = 300\text{ K}$, in the range of $0.123\text{--}1.374\text{ THz}$: the transmission decreases by about 4 orders of magnitude and the reflection increases at most four times when the material is densified. Second, figure 4 depicts the extracted SER (figure 4(a)), SEA (figure 4(b)) and SE (figure 4(c)) versus frequency (in THz) at $T = 300\text{ K}$, in the range of $0.123\text{--}1.374\text{ THz}$, for both as-grown and densified aero-GaN. It is apparent that SER is much smaller than SEA, the former in the range $0.02\text{--}0.123\text{ dB}$ and the latter spanning the range $12.51\text{--}68.23\text{ dB}$. As a result, we conclude that the total SE is due (practically) entirely to the absorption contribution (SEA). Moreover, it can be tuned by compressing the GaN.

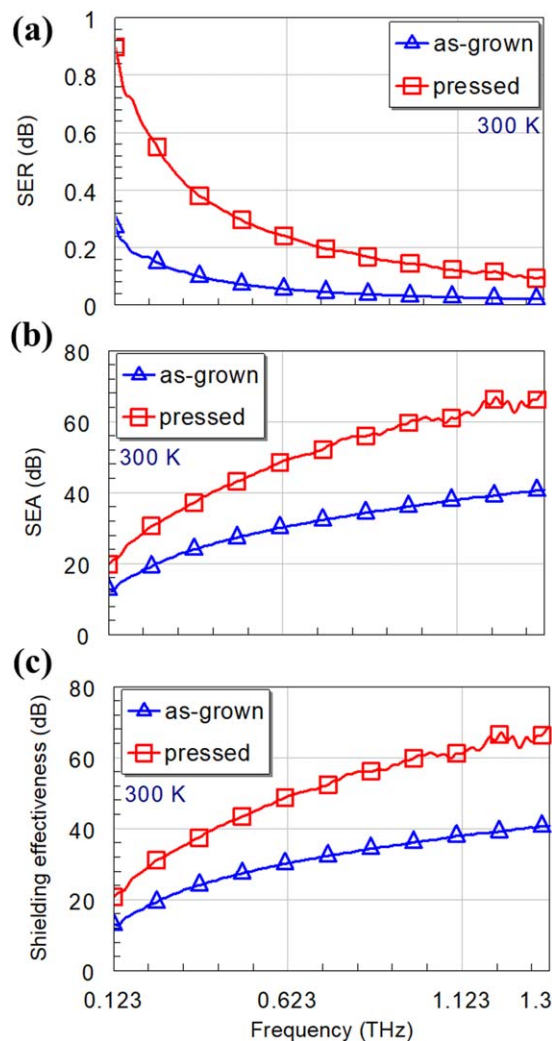


Figure 4. Extracted (a) SER, (b) SEA and (c) SE versus frequency at room temperature ($T = 300$ K), for the aero-GaN as-grown and pressed.







4. Conclusions

In this study, we have experimentally determined the spectra of electrodynamic characteristics of the aero-GaN in the THz region, at frequencies $4\text{--}100\text{ cm}^{-1}$ and temperatures $4\text{--}300$ K: real and imaginary parts of the index of refraction, dielectric permittivity and surface impedance. Basing on the measured transmission and reflection coefficients of the samples, we show that the shielding effectiveness of pressed aero-GaN exceeds 40 dB in the range $0.25\text{--}1.37$ THz being among the best THz shields known today. We point out that the value of 40 dB is required for industrial applications and is fulfilled in a huge frequency bandwidth of 1.12 THz. We note also that the aero-GaN is an ultralight, hydrophobic and chemically stable making the material attractive for various applications in electronics.

Acknowledgments

TB, VC, SR and IT acknowledge the support from the Ministry of Education, Culture and Research, Moldova, under the grants #15.817.02.29 A and #15.817.02.34 A, as well as from the European Commission under the grant #810652 ‘NanoMedTwin’. MD, MA, DD and SI acknowledge the financial support of the GRAPHENEFERRO grant of UEFISCDI, project no. PN-III-P4-ID-PCCF-2016-0033. SZ, LA and BG acknowledge support from the Ministry of Education and Science of the Russian Federation (Program 5 top 100). SS and RA acknowledge the support by the Deutsche Forschungsgemeinschaft (DFG) in the framework of SFB 677 project C-14 and SFB 1261 project A5.

ORCID iDs

Tudor Braniste  <https://orcid.org/0000-0001-6043-4642>
 Mircea Dragoman  <https://orcid.org/0000-0001-6886-5295>
 Liudmila Alyabyeva  <https://orcid.org/0000-0001-8238-4674>
 Martino Aldrigo  <https://orcid.org/0000-0003-2257-1966>
 Daniela Dragoman  <https://orcid.org/0000-0003-4241-0000>
 Sergiu Iordanescu  <https://orcid.org/0000-0001-9471-6306>
 Ion Tiginyanu  <https://orcid.org/0000-0003-0893-0854>

References

- [1] Gorshunov B, Volkov A, Spektor I, Prokhorov A, Mukhin A, Dressel M, Uchida S and Loidl A 2005 *Int. J. Infrared Millim. Waves* **26** 1217
- [2] van Slageren J *et al* 2003 *Phys. Chem. Chem. Phys.* **5** 3837
- [3] Kasagi K, Suzuki S and Asada M 2019 *J. Appl. Phys.* **125** 151601
- [4] Deal W, Mei X B, Leong K M K H, Radisic V, Sarkozy S and Lai R 2011 *IEEE Trans. Terahertz Sci. Technol.* **1** 25
- [5] Mei X *et al* 2015 *IEEE Electron. Device Lett.* **36** 327
- [6] Ma J, Shrestha R, Moeller L and Mittleman D M 2018 *Appl. Phys. Lett. Photonics* **3** 051601
- [7] Betzalela N, Ishaia P B and Feldmana Y 2018 *Environ. Res.* **163** 208
- [8] Wilmsink G J and Grundt J E 2011 *J. Infrared Millim. Terahertz Waves* **32** 1074
- [9] Gorshunov B P *et al* 2017 *Carbon* **126** 544
- [10] Zhukova E S *et al* 2017 *Nanotechnology* **28** 445204
- [11] Cervetti C, Heintze E, Gorshunov B, Zhukova E, Lobanov S, Hoyer A, Burghard M, Kern K, Dressel M and Bogani L 2015 *Adv. Mater.* **27** 2635
- [12] Liu L, Das A and Megaridis C M 2014 *Carbon* **69** 1
- [13] Tiginyanu I *et al* 2019 *Nano Energy* **56** 759
- [14] Bernardini F, Fiorentini V and Vanderbilt D 1997 *Phys. Rev. B* **56** R10024
- [15] Bernardini F and Fiorentini V 1998 *Phys. Rev. B* **57** 9427
- [16] Nishida T and Kobayashi N 2001 *Phys. Status Solidi a* **188** 113
- [17] Schulz R B, Plantz V C and Brush D R 1988 *IEEE Trans. Electromagn. Compat.* **30** 187
- [18] Al-Saleh M H and Sundararaj U 2009 *Carbon* **47** 1738

- [19] Dragoman M, Braniste T, Iordanescu S, Aldrigo M, Raevschi S, Shree S, Adelung R and Tiginyanu I M 2019 *Nanotechnology* **30** 34LT01